Comprehensive analysis of mobile genetic elements in the gut microbiome reveals phylum-level niche-adaptive gene pools

Xiaofang Jiang[1,2,†], Andrew Brantley Hall[2,3,†], Ramnik J. Xavier[1,2,3,4], and Eric Alm[1,2,5,*]

[1] Center for Microbiome Informatics and Therapeutics, Massachusetts Institute of Technology, Cambridge, MA 02139, USA

[2] Broad Institute of MIT and Harvard, Cambridge, MA 02142, USA

[3] Center for Computational and Integrative Biology, Massachusetts General Hospital and Harvard Medical School, Boston, MA 02114, USA

[4] Gastrointestinal Unit and Center for the Study of Inflammatory Bowel Disease, Massachusetts General Hospital and Harvard Medical School, Boston, MA 02114, USA

[5] MIT Department of Biological Engineering, Massachusetts Institute of Technology, Cambridge, MA 02142, USA

[†] Co-first Authors

* Corresponding Author

Abstract

Mobile genetic elements (MGEs) drive extensive horizontal transfer in the gut microbiome. This transfer could benefit human health by conferring new metabolic capabilities to commensal microbes, or it could threaten human health by spreading antibiotic resistance genes to pathogens. Despite their biological importance and medical relevance, MGEs from the gut microbiome have not been systematically characterized. Here, we present a comprehensive analysis of chromosomal MGEs in the gut microbiome using a method called Split Read Insertion Detection (SRID) that enables the identification of the exact mobilizable unit of MGEs. Leveraging the SRID method, we curated a database of 5600 putative MGEs encompassing seven MGE classes called ImmeDB (Intestinal microbiome mobile element database) (https://immedb.mit.edu/). We observed that many MGEs carry genes that confer an adaptive advantage to the gut environment including gene families involved in antibiotic resistance, bile salt detoxification, mucus degradation, capsular polysaccharide biosynthesis, polysaccharide utilization, and sporulation. We find that antibiotic resistance genes are more likely to be spread by conjugation via integrative conjugative elements or integrative mobilizable elements than transduction via prophages. Additionally, we observed that horizontal transfer of MGEs is extensive within phyla but rare across phyla. Taken together, our findings support a phylum level niche-adaptive gene pools in the gut microbiome. ImmeDB will be a valuable resource for future fundamental and translational studies on the gut microbiome and MGE communities.

Keywords: gut microbiome, mobile genetic elements, niche-adaptive, integrative conjugative elements, integrative mobilizable elements, horizontal gene transfer

35 # Introduction

36 Horizontal gene transfer (HGT), the transfer of genes between organisms by means other than vertical
37 transmission, allows for the rapid dissemination of genetic innovations between bacteria[1]. Ecology is an
38 important factor shaping HGT, and the human gut in particular is a hotspot for HGT[2,3]. HGT impacts
39 public health through its role in spreading antibiotic resistance genes[4,5]. The biological importance of
40 HGT is exemplified by a porphyranase identified in *Bacteroides plebius* that digests seaweed, which was
41 horizontally transferred from marine bacteria to human gut bacteria[6]. However, a major contributor to
42 horizontal transfer - mobile genetic elements (MGEs) - have not been systematically characterized in the
43 human gut microbiome.
44 Canonical classes of MGEs includes prophages[7], group II introns[8], and transposons[9]. It has become
45 increasingly apparent that the acquisitions of a novel element class, genomic islands correspond to HGT
46 events that differentiate commensal and pathogenic strains[10]. Genomic islands are non-canonical classes
47 of MGEs that can transfer by conjugation or genomic regions derived from such MGEs. Integrative
48 conjugative elements (ICEs) are a type of genomic island that can integrate into and excise from genomes
49 using integrase, circularize using relaxase, replicate, and then transfer via conjugation[11,12]. Integrative
50 mobilizable elements (IMEs) encode an integrase and relaxase for circularization like ICEs, but they have
51 to hijack the conjugative machinery of co-resident ICEs or conjugative plasmids[13].
52 Conventionally, HGTs are computationally identified by searching for the inconsistencies in the
53 evolutionary history of gene and species[14]. However, this method overlooks the fact the horizontal
54 transfer of multiple genes from the same locus might be the result of a single HGT event. Rather than
55 individual genes, it is critical to identify the mobilizable units, in other words, the entire sequence of
56 MGEs. Determining the mobilizable unit of MGEs is crucial to identify the mechanism of transfer, the
57 preference of insertion sites, and cargo genes as well as to track the frequency of horizontal transfer
58 events. In addition, information on MGEs are also valuable in the context of metagenomic analysis, as

59 MGEs confound many metagenomics workflows such taxonomic profiling, strain-level variation
60 detection, and pangenome analysis.
61 The repetitive and mobile nature of MGEs confounds many types of studies in microbiome communities,
62 such as taxonomic profiling, strain-level variation detection, and pan-genome analyses. However, unlike
63 research in eukaryotes, where multiple repeats databases exist for masking and annotation of repetitive
64 DNA[15], only a limited number of databases dedicated to the collection of MGE in prokaryotes[16–19] . Yet,
65 these database are either limited one specific class of MGE or obsolete and not applicable for microbiome
66 research. With the growing deluge of microbiome metagenomic sequencing data, a comprehensive MGE
67 database of the gut microbiome is becoming increasingly critical.
68 In this study, we sought to characterize MGEs from the gut microbiome to understand how horizontal
69 gene transfer by MGEs shapes the evolution of bacteria in the gut microbiome. First, we developed a
70 method to identify the exact mobilizable unit of active MGEs using whole metagenome sequencing data
71 together with references genomes. The algorithm implemented in SRID is similar to that of Daisy[20], the
72 first mapping-based HGT detection tool to our knowledge. Unlike Daisy, SRID was designed for use in a
73 metagenomic context and doesn't require pre-existing knowledge of both acceptor and donor genomes.
74 We systematically identified MGEs with SRID and curated a database named ImmeDB (Intestinal
75 microbiome mobile element database) dedicated to the collection, classification and annotation of these
76 elements. The database is organized into seven MGE classes. Each MGE entry provides a visualization of
77 annotations and downloadable genomic sequence and annotation. We detected many MGEs carrying
78 cargo genes that confer an adaptive advantage to the gut environment. We also found that conjugation via
79 integrative conjugative elements/ integrative mobilizable elements is more important than transduction
80 via prophage for the spread of antibiotic resistance genes. This study provides insights into how the
81 interplay of MGEs, bacteria, and the human host in the gut ecosystem lead to community-wide
82 adaptations to the gut environment. The curated database of MGEs we have assembled here can be used
83 by metagenomic workflows to improve future microbiome studies.

Results

Prevalence of MGEs in species of the gut microbiome

We systematically identified active MGEs from species of the human gut microbiome using mapping information from metagenomic reads from the Human Microbiome Project (HMP)[21]. MGEs are actively inserted and deleted from genomes, causing differences between strains of bacteria. We found cases where the reference genome of a bacterial strain differed from strains in the individual samples from the HMP. To find the sequences responsible for these differences, we mapped HMP metagenomic reads to available gut-associated bacterial reference genomes and identified genomic regions flanked by split reads and discordantly-aligned paired-end reads (Figure 1A). These regions potentially are recent insertions of active MGEs. The MGEs identified with the SRID method are limited to chromosomal MGEs. Thus, plasmids and extrachromosomal prophages were not characterized in this study. By searching for MGE-specific gene signatures, we verified and classified these MGEs (See Figure 1B and Methods).

We identified 5600 putative MGEs from gut microbiome representatives of 84 strains of Actinobacteria (10 species), 280 strains of Bacteroidetes (97 species), 158 strains of Firmicutes (118 species), 14 strains of Proteobacteria (12 species), and five strains of Verrucomicrobia (4 species) (Supplementary Table 2; Supplementary Data 1). Then, we classified the identified MGEs based on their transfer and transposition mechanisms into seven classes: ICEs, prophages, IMEs, group II introns, transposons, unclassified islets, and unclassified genomic islands (Figure 1C). Most of the MGEs identified (5145/5600) were from the phyla Bacteroidetes and Firmicutes because these two phyla tend to dominate the gut microbiome of healthy adults[21]. In general, smaller elements, such as transposons, had higher copy numbers per genome while larger elements, such as ICEs, prophages, and unclassified genomic islands, had a maximum of two copies per genome (Supplementary Figure 1).

Different strains of the same species often share identical or nearly-identical MGEs. To eliminate this redundancy, we collapsed MGEs into clusters based on overall nucleotide identity (Figure 1C). Phylum-level differences in the diversity of MGEs were revealed. For example, Bacteroidetes had more diversity

109 of ICEs than Firmicutes (45 vs. 26 respectively), while Firmicutes had more diversity of prophages than
110 Bacteroidetes (49 vs. 20 respectively).

111 Diversity of MGE modules in gut microbiota

112 Although it has been known that ecology is important in shaping MGEs in the gut microbiome, this study
113 is the first to systematically characterize the mechanisms of transposition and transfer for MGEs of the
114 gut microbiome[2]. We annotated the genes in MGEs involved in their transposition and transfer, and then
115 classified the elements into groups based on these annotations (Supplementary Table 2; Supplementary
116 Data 2).
117 There are four major protein families responsible for transposition of gut MGEs: serine integrases,
118 tyrosine integrases, DDE transposases, and group II intron proteins conferring reverse transcriptase and
119 endonuclease activity. Serine and tyrosine integrases are the most prevalent protein families responsible
120 for transposition in ICEs, IMEs, and prophages. In the gut microbiome MGE clusters we identified, we
121 found 315 MGEs with tyrosine integrases (54 from ICEs, 206 from IMEs and 55 from prophages) and
122 110 MGEs with serine integrases (18 from ICEs, 67 from IMEs and 25 from prophages). Interestingly,
123 while tyrosine integrases are found in several phyla, serine integrases of ICEs and prophages were
124 exclusively found in the phylum Firmicutes. In IMEs, most serine integrases were identified in
125 Firmicutes, but 10 clusters of serine integrases were found in Bacteroidetes and Actinobacteria (9 and 1
126 respectively). No ICEs and IMEs with DDE transposase were identified in our study. Nine prophage
127 clusters were found with DDE transposase from IS families: IS30, IS256, and IS110. Interestingly, all
128 three IS families use copy-paste mechanisms generating a transient double-stranded circular DNA
129 intermediate to facilitate transposition[22]. This suggests that transient double-stranded circular
130 intermediates may be essential for the life cycle of many prophages. All transposons we identified utilized
131 DDE-transposase. We identified 19 families of transposase. Most of the transposase clusters we identified
132 are present in insertion sequences. Seven clusters (28 copies) of transposons are composite transposons
133 flanked by two different insertion sequences families.

134 ICEs and IMEs encode relaxases (MOB) to initiate DNA mobilization and transfer. We used the
135 CONJscan-T4SSscan server to classify relaxases identified in MGEs[23]. Seven types of relaxase were
136 identified in ICEs and IMEs. In ICEs, MOB_T was identified only in Firmicutes, MOB_V was identified
137 only in Bacteroidetes, and MOB_{P1} was identified in Firmicutes, Bacteroidetes, and Actinobacteria. IMEs
138 have a more diverse reservoir of relaxases. Besides the three types of relaxase found in ICEs, we also
139 identified IMEs with MOB_{P3}, MOB_B, MOB_F, and MOB_Q type relaxases.
140 ICEs are capable of conjugation via mating pair formation systems. Six types of mating pair formation
141 systems for conjugation have been described[23]. We found three types of mating pair formation system:
142 typeB, typeFA, and typeFATA, in ICEs from the gut microbiome. Consistent with previous findings, type
143 FA systems were identified in 7 ICE clusters from Firmicutes, type B systems were identified in 45 ICE
144 clusters from Bacteroidetes, and type FATA systems were identified in 19 Firmicutes ICE clusters and
145 one Actinobacteria ICE cluster[24].

146 MGEs carry niche-adaptive genes

147 Although fundamentally selfish, MGEs often carry genes other than those necessary for their
148 transposition and transfer, sometimes referred to as cargo genes[25]. We found that smaller elements like
149 transposons generally carry zero or only a few cargo genes. Genetic islands like ICEs and IMEs often
150 carry numerous cargo genes (median cargo genes 44 and 12 respectively). One example is an ICE found
151 in *Bacteroides sp. 2_1_56FAA* (NZ_GL945043.1:1512740-1656974) which carries 139 cargo genes. We
152 performed functional annotation on the cargo genes, and enrichment analysis using gene ontology (GO),
153 Pfam, and Resfam[26–28] (Supplementary Table 4). Several classes of enriched genes are well-known to be
154 associated with the maintenance of MGEs such as restriction-modification systems and toxin-antitoxin
155 pairs (Supplementary Table 4). Many other gene families carried by MGEs may confer an adaptive
156 advantage to colonize the gut.

157 Antibiotic resistance genes

158 Many classes of antibiotics consumed orally are incompletely absorbed in the small intestine, and
159 therefore proceed to the large intestine where they can kill the resident microbes[29]. Therefore, genes that
160 confer antibiotic resistance can be adaptive to the gut environment. In total, we identified 781 antibiotic
161 resistance genes encompassing 46 distinct classes carried by MGEs. Classes of MGEs varied in their
162 carriage of antibiotic resistance genes. Of 8151 prophage cargo genes, only 13 were found to be antibiotic
163 resistance genes. The carriage rate of antibiotic resistance genes normalized by total cargo genes in
164 prophages is more than ten times lower than that identified in ICEs (330/16820) and IMEs (229/11053)
165 (Supplementary Figure 1). This suggests that conjugation via ICE/IME may be more important than
166 transduction in the spread of antibiotic resistance genes, consistent with previous findings[30,31].
167 GO analysis revealed that cargo genes from the class "rRNA modification" (GO:0000154), which confers
168 resistance to a wide range of antibiotics including tetracycline and erythromycin, are enriched in both
169 Bacteroidetes and Firmicutes. Resfam enrichment analysis also supported this, as RF0135 (tetracycline
170 resistance ribosomal protection protein), and RF0067 (Emr 23S ribosomal RNA methyltransferase) were
171 enriched. Other enriched antibiotic resistance gene classes carried by MGEs confer resistance to
172 chloramphenicol (RF0058), cephalosporins (RF0049) and aminoglycosides (RF0167).
173 One example of an MGE responsible for the transmission of antibiotic resistance is the ICE CTnDOT, the
174 spread of which dramatically increased the prevalence of tetracycline-resistant Bacteroidetes species[32].
175 CTnDOT-like ICEs were clustered in ICE1. Elements in this cluster typically confer resistance to
176 tetracycline via the tetQ antibiotic resistance gene (Figure 2A). In addition, ICE1 elements have multiple
177 sites where antibiotic resistance genes can be inserted or substituted. We characterized 5 insertions of
178 antibiotic resistance genes into ICE1 (Figure 2A). Insertion sites 1, 2, and 5 are between operons;
179 therefore they do not interrupt the function of crucial genes. We observed one insertion and two
180 substitutions of antibiotic resistance genes around the tetQ operon, suggesting that this site is likely a
181 "hotspot" for insertions and substitutions of antibiotic resistance genes. Our analysis reveals the

182 surprising extent to which MGEs in species of the gut microbiome contribute to the phenomenon of
183 antibiotic resistance and that the insertion of antibiotic resistance genes into MGEs is an active and
184 ongoing process.

185 ## Bile salt hydrolase and bile transporters

186 Bile acids are found in high concentrations in the human intestines[33] and can be toxic to bacteria[34].
187 Therefore, gut microbes have developed strategies to deal with bile acids by actively pumping bile acids
188 out of the cell, or via deconjugation, which is hypothesized to diminish the toxicity of bile acids[33,34]. The
189 high identity of archaeal and bacterial bile salt hydrolases strongly suggests the horizontal transfer of this
190 gene[35]. A sodium bile acid symporter family (PF01758), which could help to pump bile acids out of the
191 cell, was found to be enriched in the cargo genes of MGEs. Furthermore, 61 examples of bile salt
192 hydrolases were identified as cargo genes of MGEs (Supplementary Table 3). Thus, MGEs carry genes
193 that help microbes to overcome a specific challenge of colonizing the human gut.

194 ## Glycoside hydrolases for mucus utilization

195 The colon is lined with a layer of mucus composed of the glycoprotein MUC2[36]. The glycans that
196 decorate MUC2 have a core structure composed of galactose, N-acetylglucosamine, N-
197 acetylgalactosamine, with terminal residues of fucose and sialic acid[37]. These specific glycans are a major
198 energy source for members of the gut microbiota[38]. Therefore, it may benefit members of the gut
199 microbiota to degrade these specific glycans[39]. We found cargo genes carried by MGEs from
200 Bacteroidetes species were enriched for GO:0004308, an exo-sialidase involved in the degradation of
201 mucosal glycans. In addition, we identified 60 glycoside hydrolases capable of degrading mucosal
202 glycans carried by MGEs from the categories: sialidases (GH33), fucosidases (GH95), α-N-
203 acetylgalactosaminidases (GH109), and β-galactosidases (GH20)[38,40] (Supplementary Table 3). Thus,
204 MGEs carry genes to unlock a key energy source available to gut microbes.

205 ## Polysaccharide Utilization Loci

206 Gut Bacteroidetes can utilize a wide variety of polysaccharides via the products of polysaccharide
207 utilization loci, which collectively make up large proportions of Bacteroidetes genomes[41]. Each
208 polysaccharide utilization locus contains a copy of the gene SusC, a sugar transporter, and SusD, a glycan
209 binding protein[42]. Due to the wide range of polysaccharides available to gut microbes, it is hypothesized
210 that the possession of a large repertoire of polysaccharide utilization loci confers an adaptive advantage in
211 Bacteroidetes[41]. We found 43 polysaccharide utilization loci containing both SusC and SusD carried by
212 MGEs suggesting that the ability to degrade complex polysaccharides may be readily transferred between
213 members of the gut microbiota (Supplementary Table 3).

214 ## Capsular Polysaccharide Biosynthesis Loci

215 Many bacterial species produce capsules, an extracellular structure made up of polysaccharides[43].
216 However, gut Bacteroidetes species have a large repertoire of capsular polysaccharide biosynthesis loci
217 (up to 8) compared to other bacterial species and even Bacteroidetes from other sites such as the mouth[44].
218 Furthermore, capsular polysaccharide biosynthesis loci have been reported to be the most polymorphic
219 region of *Bacteroides* genomes[45,46]. Multiple capsular polysaccharide biosynthesis loci are necessary to
220 competitively colonize the gut, and are therefore considered to be gut adaptive genes in gut
221 Bacteroidetes[47].
222 Capsular polysaccharide biosynthesis loci are large and complex; many contain upwards of 20 genes[43].
223 We found 21 complete or fragmented capsular polysaccharide biosynthesis loci containing at least 10
224 genes carried by MGEs (Supplementary Table 3). For example, almost identical copies of ICE9
225 containing a capsular polysaccharide biosynthesis locus were found in two species, *B. stercoris* and *B. sp.*
226 *UW*. The same capsular polysaccharide biosynthesis locus was also found in *B. vulgatus,* but the ICE9
227 copy was slightly divergent. Two other copies of ICE9 likely containing an orthologous capsular
228 polysaccharide biosynthesis locus were also found in *B. fragilis* and *B. sp. 9_1_42FAA* (Figure 2B).
229 Additionally, many GO-terms related to capsular polysaccharide biosynthesis are enriched in

230 Bacteroidetes MGEs including GO:0045226, GO:0034637, GO:0044264, and GO:0000271. A Pfam for
231 glycosyltransferases involved in the biosynthesis of capsular polysaccharides (PF13579) was enriched in
232 Bacteroidetes MGEs. The transfer of large segments of capsular polysaccharide biosynthesis loci by
233 MGEs may help to explain the incredible diversity of capsular polysaccharide biosynthesis loci observed
234 in the genomes of gut Bacteroidetes[48].

235 Sporulation

236 The gut is an anaerobic environment colonized by many classes of strictly anaerobic organisms[49,50].
237 However, to transmit between hosts, gut microbes must be exposed to oxygen. Recent work has shown
238 that many more gut microbes form spores than previously thought, likely enabling transmission between
239 hosts[51]. In Firmicutes, 14 genes involved in sporulation (GO:0030435) were found to be enriched in
240 MGEs. In addition, PF08769 (Sporulation initiation factor Spo0A C terminal) and PF04026 (SpoVG)
241 were also enriched in our Pfam analysis.
242 One example is GI153, a genetic island from *Faecalibacterium prausnitzii A2-165*, which contains a
243 series of spore formation-related genes in an operon: SpoVAC, SpoVAD, spoVAEb, gpr (spore protease),
244 and spoIIP. Another example is GI175, a genetic island derived from a degenerate prophage in *Roseburia*
245 *intestinalis* L1-82. In one operon of GI175, there are three genes: SpoVAEb, SpoVAD, and one unknown
246 gene with Cro/C1-type HTH DNA-binding domain. SpoVAC, SpoVAD, spoVAEb homologs were
247 previously found to be carried by a Tn1546-like ICE and conferred heat resistance to spores in the model
248 spore forming organism *Bacillus subtilis*[52]. Thus, MGEs may help to transfer genes involved in
249 sporulation between gut microbiota which may prove adaptive for colonizing new hosts.

250 Summary of cargo genes

251 Many additional gene families were found to be enriched in MGEs that could plausibly be niche adaptive
252 including: histidine sensor kinases, and genes involved in vitamin B biosynthesis (Supplementary Table
253 4). Notably, MGEs from Firmicutes and Bacteroidetes have different types of genes enriched reflecting

254 the differences in physiology between the phyla. Antibiotic resistance genes and genes involved in the
255 detoxification of bile acids are enriched in MGEs from both phyla. Glycoside hydrolases for mucus
256 utilization, and capsular polysaccharide biosynthesis loci are enriched only in MGEs from Bacteroidetes,
257 while genes for sporulation are enriched in MGEs only from Firmicutes. Overall, the transfer of niche
258 adaptive genes by MGEs likely has a large impact on the fitness of species of the gut microbiome.

259 Host ranges and evolution of MGEs

260 Although MGEs readily transfer between species, there has not been a systematic analysis of the host
261 range of MGEs in the gut microbiome. The host ranges of different classes of MGEs is variable, and even
262 within a class, different elements have variable host ranges. Understanding the host range of gut MGEs is
263 of particular importance because gut MGEs carry many cargo genes, and the host range of the MGE
264 defines how widely these cargo genes can be distributed. For example, the gut microbiome is a reservoir
265 of antibiotic resistance genes, and many antibiotic resistance genes are located within MGEs[53]. Therefore,
266 it is important to understand the probability of the transfer of MGEs with antibiotic resistance genes from
267 commensals to pathogens[53].
268 First, we studied the host range of MGEs from the same cluster. MGEs in the same cluster that exist in at
269 least two species generally represent recent horizontal transfer. Some MGE clusters are present in a wide
270 range of species indicative of active horizontal transfer. One example is the ICE1 cluster, a representative
271 of the CTnDOT-like ICEs, which is found in 32 species of Bacteroidetes from the genera: *Bacteroides,*
272 *Parabacteroides, Allistipes,* and *Paraprevotella* (Supplementary Figure 1). The entirety of the 49kb
273 element is found at more than 99 percent nucleotide identical to 10 *Bacteroides, Parabacteroides, and*
274 *Allistipes* species, indicative of very recent horizontal transfer. This cluster also includes other CTnDOT-
275 like elements with more variability such as CTnERL, which has an additional insertion of an IME
276 conferring erythromycin resistance[54]. Another example is the Firmicutes ICE cluster ICE10, which is
277 found in 10 species of the families *Lachnospiraceae* and *Ruminococcaceae*. This ICE10 cluster belongs
278 to Tn916/Tn1549 family of ICEs, some members of which carry the medically-important VanB gene

279 conferring resistance to vancomycin[55]. We found no examples of ICEs from the same cluster present in
280 multiple phyla. Clusters of prophage, IMEs, group II introns, and transposons were also found in many
281 species but were again limited to a single phylum. Our results support that although the recent horizontal
282 transfer of MGEs is common within phyla, cross-phyla horizontal transfer is rare, as we did not observe
283 any cross-phyla horizontal transfer events for elements of the same cluster.
284 Here we generated phylogenetic trees of tyrosine and serine integrases from ICEs and prophages
285 identified to study the evolutionary history of the recombination module of MGEs. To contrast the
286 phylogeny of the tyrosine and serine integrases with host species lineages we plotted tanglegrams (Figure
287 3 and Figure 4). The phylogeny of both the serine and tyrosine integrases is incongruent with the host
288 species lineages which is indicative of extensive past horizontal transfer of ICEs and prophages between
289 species of the gut microbiome.
290 The tyrosine integrases can be divided into two clades: the first is associated with the phylum
291 Bacteroidetes, the second clade is associated with the phyla Proteobacteria, Actinobacteria, Firmicutes
292 and Verrucomicrobia (Figure 3). Tyrosine integrases from Bacteroidetes show no evidence of close inter-
293 phyla transfer but ancient transfers of tyrosine integrases between the phyla Proteobacteria,
294 Actinobacteria, and Firmicutes likely occurred several times during evolution. Serine integrases from
295 ICEs and prophages were only found in the phylum Firmicutes. Therefore, we found no evidence of inter-
296 phyla transfer for ICEs and prophages with serine integrases suggesting a phylum-level restriction in host
297 range.
298 We also examined whether integrases derived from ICEs and prophages segregated into clades based on
299 element type. Previous studies on the phylogenetic relationships of integrases from ICEs and prophages
300 did not find strong evidence of intermingling between ICE and prophage integrases[56,57]. In our phylogeny
301 of the tyrosine integrases, ICE and prophage integrases are extensively intermingled, suggesting that ICEs
302 and prophages have exchanged integrases multiple times over the course of evolution. Moreover, in our
303 phylogeny of serine integrases, ICE22 and ICE64 appear in a branch containing mostly prophages,
304 suggesting that the integrase may have originated from a prophage integrase.

305 Unlike prophages and ICEs, 8 of 67 clusters of IMEs use serine integrases to transpose in Bacteroidetes.
306 This implies that although integration via serine integrases occurs in Bacteroidetes, it occurs much less
307 frequently than integration via tyrosine integrases. For transposons, 17 out of 19 transposase families
308 were found in species from different phyla, indicating an extensive history of ancient horizontal transfer.
309 Based on the tanglegram of group II intron proteins, no phylum corresponds to a single clade of group II
310 introns, indicating cross-phyla horizontal transfers during the evolution of group II introns in the gut
311 microbiome (Supplementary Figure 2).
312 In summary, although ancient cross-phyla horizontal transfers did occur during the evolution of MGEs,
313 we did not observe recent cross-phyla horizontal transfer of MGEs. Therefore, the gene pools that are
314 shared within the gut microbiome are likely limited to the phyla-level.

315 Modular evolution of gut MGEs

316 Genes in MGEs are typically organized in functionally related modules which can be readily exchanged
317 between MGEs. Type of modules found in MGEs include: conjugation, integration, regulation, and
318 adaptation. Deletion, acquisition, and exchanges of these modules can lead to immobilization, adaptation,
319 and shifts in insertion specificity and host ranges of MGEs[13]. Here, we detail examples of each of these
320 types of events.
321 Many unclassified genetic islands are likely remnants of ICEs or prophages due to the presence of only a
322 subset of genes necessary for autonomous transfer. In many cases, the integrase have been lost while
323 other genes for conjugation or capsid formation are maintained. One example is GI73, which appears to
324 have formed when a CTnDOT-like element lost its conjugation and mobilization modules to a large
325 deletion (Figure 5A). We also observed many examples of the acquisition of new modules by insertions.
326 CTnDOT-like elements have obtained adaptive modules via insertions of a group II intron together with
327 the antibiotic resistance gene ErmF, an IME containing multiple antibiotic resistance genes including:
328 ANT6, tetX, and ErmF[54,58], and other unidentified insertions containing many antibiotic resistance genes
329 (Figure 2A; Supplementary Data 3; Supplementary Table 5). Other examples are GI90, where ICE7

330 (CTnBST) inserted into a CTnDOT-like element (Figure 5A), and GI46, a genomic island formed when
331 two types of ICEs (ICE43 and ICE56) inserted in tandem (Figure 5B). We observed that the exchange of
332 recombination modules is common. Integrases have frequently been exchanged between ICEs and
333 prophages during the evolution of MGEs (Figure 3 and Figure 4). Exchanges also occur in the same class
334 of MGE. For example, we observed that two clusters of ICEs, ICE15 and ICE16, share nearly identical
335 sequences and the same typeFA conjugation module, but have different integrases: ICE15 has a tyrosine
336 integrase while ICE16 has a serine integrase (Figure 5C). Overall, the modular nature of MGEs enables
337 the formation of new mosaic elements, leading to the diversification of MGEs, and increasing the
338 dynamics of the gene pools in the gut microbiome.

339 Discussion

340 In this study, we systematically characterized MGEs from the gut microbiome using a novel method to
341 identify the mobilizable unit of active MGEs. We dramatically expanded the number of annotated MGEs
342 from gut microbial species by identifying 5600 putative MGEs. The MGEs we identified allows for the
343 understanding of several fundamental questions about the role of MGEs and their importance to the
344 evolution of species of the gut microbiome.

345 Implications for future gut metagenomic analysis

346 The database of MGEs we have curated will be a valuable resource for future studies on the gut
347 microbiome, especially with the increasing importance of taxonomic profiling, strain-level variation
348 detection, and pangenome analyses. Many metagenomic workflows for taxonomic profiling use marker
349 genes or k-mers "unique" to a specific species, where uniqueness is constrained by the available
350 reference genomes[59–61]. These marker gene should exclude MGEs, as the potential horizontal transfer of
351 these elements invalidates their "unique" species-specific associations. Strain-level variation analyses that
352 based on single nucleotide polymorphisms (SNPs) or copy number variation should also exclude SNPs

353 from MGEs[62–65]. In pangenome analysis, it is beneficial to distinguish the accessory genes unique to an
354 individual species and the mobilome shared among multiple species. To address the problems posed by
355 MGEs to metagenomic workflows, an approach common in eukaryotic genomics, repeat masking, can be
356 applied[66,67]. The database of curated MGEs identified in this study can be used to mask gut microbiome
357 reference genomes before metagenomic workflows such as species-level classification, strain-level
358 detection, and pangenome analyses are performed.

359 Host ranges of MGEs and the spread of antibiotic resistance genes

360 In the United States alone, more than 23,000 people die each year from antibiotic-resistant infections[68].
361 Tracking antibiotic resistance is one of the key actions to fight the spread of antibiotic resistance. The
362 human digestive tract is a major reservoir of antibiotic resistance genes and likely serves as a hub for the
363 horizontal transfer of antibiotic resistance genes from commensals to pathogens[4,5,53]. MGEs play a
364 significant role in the spread of antibiotic resistance genes, and we found that many MGEs in the gut
365 microbiome contain antibiotic resistance genes. This study helps to define the host range of MGEs in the
366 gut microbiome. Our results suggest that HGT occurs mostly within a phylum, and inter-phyla HGT is
367 rare. These results underscore the risk posed by transfer of antibiotic resistance genes like the
368 vancomycin-resistance conferring gene VanB between commensal Firmicutes and pathogenic Firmicutes,
369 such as *Enterococcus faecalis*[69]. Overall, our study advances the understanding of the host range of MGEs
370 which is of critical importance to understand gene flow networks in the gut.
371
372 This study underestimates the extent of host range because only MGEs in sequenced genomes were
373 detected. As more bacterial genomes are sequenced, the extent of host range of MGEs will be refined.
374 The scope of our research is chromosomal MGEs. Thus, plasmids or prophages existing as an
375 extrachromosomal plasmid were not characterized in this study. Future studies using a combination of
376 molecular and computational approaches are beneficial to further understand the rate and extent of
377 horizontal gene transfer by MGEs.

Niche-adaptive genes in the communal gene pool

The mammalian gut is a unique ecological niche vastly different from other environments due to the presence of IgA, antimicrobial peptides, bile acids, as well as specific polysaccharides available for utilization in the intestinal mucus. The microbes that inhabit the gut must develop mechanisms to cope with these challenges. We observed that MGEs transfer genes to help address the unique challenges of colonizing the human gut. MGEs influence the spread of gut adaptive genes in three ways. First, the spread of MGEs drives the expansion and diversification of protein families such as those involved in polysaccharide utilization, capsular polysaccharide biosynthesis, and sensing and responding to the environment[9]. Second, MGEs transfer successful innovations for colonizing the gut among distantly-related species from the same niche, such as bile salt hydrolases. Third, MGEs allow for the amplification and transfer of genes that are adaptive only under specific conditions, such as antibiotic resistance genes, and sporulation-related genes.

Cargo genes transferred by MGEs can have wide-ranging effects on the biology of the gut microbiome. They potentially involved in bacterial symbioses, sensing and responding to environmental stimuli, and metabolic versatility. The enriched classes of cargo genes we identified in this study are attractive targets for future studies to understand the underlying biology of the gut microbiome.

Opportunities to use MGEs to engineer gut microbes

Tools for genome editing only exist for a very limited number of species of the gut microbiome despite the exceptional basic and translational opportunities afforded by engineering gut species. Many of the tools for editing the genomes of species were originally derived from MGEs. For instance, the NBU system used to modify some *Bacteroides* species was originally derived from an IME[70], and the TargeTron system was originally derived from a group II intron[71]. The novel examples of MGEs identified in this study could be used to edit genomes from the gut microbiome, especially in currently intractable species such as *Faecalibacterium prausnitzii*. Unlike phages, whose cargo genes are limited by the capsid size, many novel ICEs and IMEs carry hundreds of genes that can confer selective advantages

403 for the host, and are excellent candidate vectors for large genetic loci. Overall, the MGEs identified in this
404 study could have translational applications for genome editing of species from the gut microbiome.

405 Methods

406 Detection of putative MGEs

407 80 Samples from the Human Microbiome Project (HMP)[21] and 66,232 bacterial genomes were
408 downloaded from the NCBI (2016/09/14). We used Mash[72] to calculate the minhash distance between
409 each genome and all metagenomic samples with the default sketch size of $s = 1000$ and $k = 21$. If the
410 matching-hashes shared between a genome and the 80 metagenomic samples are less than 2, the genome
411 is unlikely have enough alignments from these samples and was removed. This steps help us quickly
412 remove genomes that likely do not exist or exist in low abundance in gut microbiome. 9,846 genomes
413 remained after this filtering step. Metagenomic reads from HMP samples were aligned to each of the
414 9,846 genome separately with bwa (version 0.7.5a-r405)[73]. To find genomic regions that differ in terms of
415 insertions/deletions between strains in the individual samples and the reference genomes, we used split
416 reads and information from pair-end reads from the alignment (Figure 1A). First, we identified putative
417 deletion junctions using split reads, which we defined as reads that align to two distinct portions of a
418 genome. Split reads were initially identified as those reads having multiple hits in the SAM output from
419 bwa. If a split read alignment starts at one genomic location in the reference and then "jumps" to aligning
420 to a distant site downstream in the same strand, it may indicate a potential deletion in the strain of bacteria
421 from the metagenomic sample compared to the reference genome. For each putative deletion junctions,
422 we confirmed the presence of the junction by determining if paired-end reads flanked the junction. We
423 considered a deletion junction to be valid if the reads pairs flanking the junction were aligned in the
424 correct orientation, and the distance between the pairs minus the junction size is within the range of +/- 2
425 times the standard deviation of the mean insertion size (202.4 +/- 2X71.5 for our data set) . Regions with

426 more than four split reads and more than four read pairs supporting the deletion were considered as
427 putative MGEs. We chose the MGEs ranging in size between 1kbp and 150kbps to reduce the number of
428 spurious results. In total, we identified MGEs in 703 genomes. The code used to implement the SRID
429 method, genome assembly accession numbers and HMP SRA accession numbers used in this study are
430 available from github (https://github.com/XiaofangJ/SRID) and the Supplementary Data 4.

431 MGE signature detection

432 Genes from the 703 genomes identified before were predicted with Prodigal (version 2.6.3)[74]. Protein
433 sequences were functionally annotated with interproscan (version 5.19-58.0) using the default settings[75].
434 Then, we used the interprosan annotations to identify serine and tyrosine integrases as well as group II
435 intron proteins from all genomes. prophage-related genes were identified by searching for genes with
436 Pfams signatures identified in phage_finder[76]. Serine integrases were identified as genes annotated with
437 the Pfam identifiers: PF00239 (Resolvase: resolvase, N terminal domain), PF07508 (Recombinase:
438 recombinase), and PF13408 (Zn_ribbon_recom: Recombinase zinc beta ribbon domain). Tyrosine
439 integrases were identified as genes annotated with the identifiers: PF00589 (Phage_integrase: site-
440 specific recombinase, prophage integrase family), PF02899 (Phage_integr_N: prophage integrase, N-
441 terminal SAM-like domain), PF09003 (Phage_integ_N: bacteriophage lambda integrase, N-terminal
442 domain), TIGR02225 (recomb_XerD: tyrosine recombinase XerD), TIGR02224 (recomb_XerC: tyrosine
443 recombinase XerC), and PF13102 (Phage_int_SAM_5: prophage integrase SAM-like domain). Group II
444 intron proteins were identified as genes annotated with the identifier: TIGR04416 (group_II_RT_mat:
445 group II intron reverse transcriptase maturase). To identify genes in involved in mobilization and
446 conjugation of MGEs, we used ConjScan via a Galaxy web server (https://galaxy.pasteur.fr/)[77]. We
447 identified transposases using blastp against the IS database with an e-value 1-e3[17]. The best hit for each
448 protein was used to annotate the family of transposases.

449 ## Classification of MGEs

450 Putative MGEs were annotated as an ICE if they contained complete conjugation and relaxase modules
451 and an integrase or DDE-transposase at the boundary of the element. Putative MGEs were annotated as
452 prophages if there is an integrase or DDE-transposase at the boundary of the element and more than five
453 genes were annotated with prophage-related Pfams. Putative MGEs were annotates as IMEs if they
454 contained an integrase or DDE-transposase and relaxase did not contain genes involved in conjugation.
455 Putative MGEs were annotated as transposons if they contained transposase and were not previously
456 annotated as an IME. We limited the size of IMEs to 30kb and transposons to 10kb to decrease the
457 number of false positives. Putative MGEs were annotated as group II introns if the element was less than
458 10kb, contained a protein with the TIGR04416 signature, and did not contain a gene annotated as
459 transposase. The remaining putative MGEs were then divided into two groups based on their sizes:
460 unclassed genomic islands (>10kb), and islets (<10kb). To eliminate spurious MGEs, we only report
461 genomic islands that contain an integrase or DDE transposase, or those that are related to prophage/ICEs,
462 and islets that exist in more than two species. After classification and verification, we identified 5600
463 MGEs in 542 genomes(Supplementary Data 1;Supplementary Data 2).

464 ## Clustering each class of MGEs

465 Pairwise alignment of elements from the same class of MGEs was performed with nucmer (version 3.1)[78].
466 Elements with more than 50 percent of the sequence aligned to each other are grouped in the same cluster.
467 For ICEs, we additionally require that elements in the same cluster should have the same types of
468 integrase, relaxase and conjugation modules. For IMEs, we required that each cluster has the same the
469 types of integrases and relaxases for all elements. For transposons, the same cluster should have the same
470 type and number of IS genes. If a transposon is a “nested” or composite transposon, the family names of
471 all IS contained within were used to annotate the transposon.

472 ## Construction of phylogenetic trees

473 To build phylogenetic trees of ICE and prophage integrases, we selected a representative integrase
474 sequence for each cluster. For group II introns, we selected a representative group II intron reverse
475 transcriptase/maturase from each cluster.The representative protein is a single protein chosen that has the
476 greatest amino acid identity, on average, to its homolog sequences of the same cluster. We performed
477 alignment of each group of sequences with mafft(v7.123b)[79] (parameter " --maxiterate 1000"). We used
478 trimal (version 1.4.rev15)[80] to remove region with gaps representing more than 20% of the total
479 alignments (parameter "-gt 0.8"). RAxML(version 8.2.10)[81] was used to build the phylogenetic trees from
480 the alignments using the LG substitution matrix and a gamma model of rate heterogeneity (parameter "-m
481 PROTGAMMALGF"). Phylogenetic trees were plotted with the R package phytools[82].

482 ## Functional enrichment analysis of cargo genes

483 Cargo genes are identified by excluding genes involved in transposition and transfer from all genes on
484 MGEs.
485 To understand the function of cargo genes, we performed enrichment analysis based on gene ontology
486 (GO), antibiotic resistance (Resfam), and protein families (Pfam). The enricments were performed with
487 all genes present in the genomes as background reference. We used hmmer[83] to search Resfam[28] database
488 to annotate antibiotic resistant gene. The "--cut_ga" parameters were used to set the threshold. The best
489 hits to each gene from the Resfam database were used to annotate antibiotic resistant genes. GO terms and
490 Pfam signature of the same genes sets were extracted from interproscan result. R package GOStat[84] was
491 used for GO enrichment analysis for GO and Pfam. The R package clusterProfiler[85] was used for the
492 enrichment analysis of cargo genes based on Resfam and Pfam signatures. P-value of 0.05 were used as
493 cutoff for all enrichment analysis.

494 ## Correspondence

495 Correspondence and requests for materials should be addressed to:

496 Eric Alm
497 Massachusetts Institute of Technology
498 Building NE47-379
499 Cambridge, MA 02139
500 ejalm@mit.edu
501 +1 617 253 2726

502 Acknowledgements

503 This work is supported by the Center for Microbiome Informatics and Therapeutics at MIT. A.B.H. is a
504 Merck Fellow of the Helen Hay Whitney Foundation.
505

506 Competing financial interests.

507 Eric Alm is a co-founder and shareholder of Finch Therapeutics, a company that specializes in
508 microbiome-targeted therapeutics. Other authors declare that they have no competing interests.

509 Authors' contributions

510 Data generation, analysis, and presentation: XJ and ABH; Writing of the manuscript: XJ, ABH; Initiated
511 the study, provided resources, tools and critical review of manuscript: RJX, EA. All authors read and
512 approved the final manuscript.

513 References

514 1. Soucy, S. M., Huang, J. & Gogarten, J. P. Horizontal gene transfer: building the web of life. *Nat.*
515 *Rev. Genet.* **16,** 472–482 (2015).
516 2. Smillie, C. S. *et al.* Ecology drives a global network of gene exchange connecting the human
517 microbiome. *Nature* **480,** 241–244 (2011).
518 3. Brito, I. L. *et al.* Mobile genes in the human microbiome are structured from global to individual
519 scales. *Nature* **535,** 435–439 (2016).
520 4. Huddleston, J. R. Horizontal gene transfer in the human gastrointestinal tract: potential spread of
521 antibiotic resistance genes. *Infect. Drug Resist.* **7,** 167–176 (2014).
522 5. Roberts, A. P. & Mullany, P. Oral biofilms: a reservoir of transferable, bacterial, antimicrobial
523 resistance. *Expert Rev. Anti. Infect. Ther.* **8,** 1441–1450 (2010).
524 6. Hehemann, J.-H. *et al.* Transfer of carbohydrate-active enzymes from marine bacteria to Japanese
525 gut microbiota. *Nature* **464,** 908–912 (2010).
526 7. Krupovic, M., Prangishvili, D., Hendrix, R. W. & Bamford, D. H. Genomics of bacterial and
527 archaeal viruses: dynamics within the prokaryotic virosphere. *Microbiol. Mol. Biol. Rev.* **75,** 610–
528 635 (2011).
529 8. Lambowitz, A. M. & Zimmerly, S. Group II introns: mobile ribozymes that invade DNA. *Cold*
530 *Spring Harb. Perspect. Biol.* **3,** a003616 (2011).
531 9. Treangen, T. J. & Rocha, E. P. C. Horizontal transfer, not duplication, drives the expansion of
532 protein families in prokaryotes. *PLoS Genet.* **7,** e1001284 (2011).
533 10. Hacker, J. & Carniel, E. Ecological fitness, genomic islands and bacterial pathogenicity. A
534 Darwinian view of the evolution of microbes. *EMBO Rep.* **2,** 376–381 (2001).
535 11. Wozniak, R. A. F. & Waldor, M. K. Integrative and conjugative elements: mosaic mobile genetic

536 elements enabling dynamic lateral gene flow. *Nat. Rev. Microbiol.* **8,** 552–563 (2010).
537 12. Johnson, C. M. & Grossman, A. D. Integrative and Conjugative Elements (ICEs): What They Do
538 and How They Work. *Annu. Rev. Genet.* **49,** 577–601 (2015).
539 13. Bellanger, X., Payot, S., Leblond-Bourget, N. & Guédon, G. Conjugative and mobilizable genomic
540 islands in bacteria: evolution and diversity. *FEMS Microbiol. Rev.* **38,** 720–760 (2014).
541 14. Ravenhall, M., Škunca, N., Lassalle, F. & Dessimoz, C. Inferring horizontal gene transfer. *PLoS*
542 *Comput. Biol.* **11,** e1004095 (2015).
543 15. Hoen, D. R. *et al.* A call for benchmarking transposable element annotation methods. *Mob. DNA* **6,**
544 13 (2015).
545 16. Arndt, D. *et al.* PHASTER: a better, faster version of the PHAST phage search tool. *Nucleic Acids*
546 *Res.* **44,** W16–21 (2016).
547 17. Siguier, P., Perochon, J., Lestrade, L., Mahillon, J. & Chandler, M. ISfinder: the reference centre for
548 bacterial insertion sequences. *Nucleic Acids Res.* **34,** D32–6 (2006).
549 18. Bi, D. *et al.* ICEberg: a web-based resource for integrative and conjugative elements found in
550 Bacteria. *Nucleic Acids Res.* **40,** D621–6 (2012).
551 19. Leplae, R., Lima-Mendez, G. & Toussaint, A. ACLAME: a CLAssification of Mobile genetic
552 Elements, update 2010. *Nucleic Acids Res.* **38,** D57–61 (2010).
553 20. Trappe, K., Marschall, T. & Renard, B. Y. Detecting horizontal gene transfer by mapping
554 sequencing reads across species boundaries. *Bioinformatics* **32,** i595–i604 (2016).
555 21. Human Microbiome Project Consortium. Structure, function and diversity of the healthy human
556 microbiome. *Nature* **486,** 207–214 (2012).
557 22. Siguier, P., Gourbeyre, E. & Chandler, M. Bacterial insertion sequences: their genomic impact and
558 diversity. *FEMS Microbiol. Rev.* **38,** 865–891 (2014).
559 23. Guglielmini, J. *et al.* Key components of the eight classes of type IV secretion systems involved in
560 bacterial conjugation or protein secretion. *Nucleic Acids Res.* **42,** 5715–5727 (2014).
561 24. Guglielmini, J., de la Cruz, F. & Rocha, E. P. C. Evolution of conjugation and type IV secretion
562 systems. *Mol. Biol. Evol.* **30,** 315–331 (2013).
563 25. Rankin, D. J., Rocha, E. P. C. & Brown, S. P. What traits are carried on mobile genetic elements,
564 and why? *Heredity* **106,** 1–10 (2011).
565 26. Ashburner, M. *et al.* Gene Ontology: tool for the unification of biology. *Nat. Genet.* **25,** 25–29
566 (2000).
567 27. Finn, R. D. *et al.* Pfam: the protein families database. *Nucleic Acids Res.* **42,** D222–30 (2014).
568 28. Gibson, M. K., Forsberg, K. J. & Dantas, G. Improved annotation of antibiotic resistance
569 determinants reveals microbial resistomes cluster by ecology. *ISME J.* **9,** 207–216 (2015).
570 29. Connelly, S. *et al.* SYN-004 (ribaxamase), an Oral Beta-Lactamase, Mitigates Antibiotic-Mediated
571 Dysbiosis in a Porcine Gut Microbiome Model. *J. Appl. Microbiol.* (2017). doi:10.1111/jam.13432
572 30. Volkova, V. V., Lu, Z., Besser, T. & Gröhn, Y. T. Modeling the infection dynamics of
573 bacteriophages in enteric Escherichia coli: estimating the contribution of transduction to
574 antimicrobial gene spread. *Appl. Environ. Microbiol.* **80,** 4350–4362 (2014).
575 31. Enault, F. *et al.* Phages rarely encode antibiotic resistance genes: a cautionary tale for virome
576 analyses. *ISME J.* **11,** 237–247 (2017).
577 32. Shoemaker, N. B., Vlamakis, H., Hayes, K. & Salyers, A. A. Evidence for extensive resistance gene
578 transfer among Bacteroides spp. and among Bacteroides and other genera in the human colon. *Appl.*
579 *Environ. Microbiol.* **67,** 561–568 (2001).
580 33. Devlin, A. S. & Fischbach, M. A. A biosynthetic pathway for a prominent class of microbiota-
581 derived bile acids. *Nat. Chem. Biol.* **11,** 685–690 (2015).
582 34. Begley, M., Gahan, C. G. M. & Hill, C. The interaction between bacteria and bile. *FEMS Microbiol.*
583 *Rev.* **29,** 625–651 (2005).
584 35. Jones, B. V., Begley, M., Hill, C., Gahan, C. G. M. & Marchesi, J. R. Functional and comparative
585 metagenomic analysis of bile salt hydrolase activity in the human gut microbiome. *Proc. Natl. Acad.*
586 *Sci. U. S. A.* **105,** 13580–13585 (2008).

36. Johansson, M. E. V. *et al.* The inner of the two Muc2 mucin-dependent mucus layers in colon is devoid of bacteria. *Proceedings of the National Academy of Sciences* **105,** 15064–15069 (2008).
37. Johansson, M. E. V., Larsson, J. M. H. & Hansson, G. C. The two mucus layers of colon are organized by the MUC2 mucin, whereas the outer layer is a legislator of host-microbial interactions. *Proc. Natl. Acad. Sci. U. S. A.* **108 Suppl 1,** 4659–4665 (2011).
38. Tailford, L. E., Crost, E. H., Kavanaugh, D. & Juge, N. Mucin glycan foraging in the human gut microbiome. *Front. Genet.* **6,** 81 (2015).
39. Li, H. *et al.* The outer mucus layer hosts a distinct intestinal microbial niche. *Nat. Commun.* **6,** 8292 (2015).
40. Lombard, V., Golaconda Ramulu, H., Drula, E., Coutinho, P. M. & Henrissat, B. The carbohydrate-active enzymes database (CAZy) in 2013. *Nucleic Acids Res.* **42,** D490–5 (2014).
41. Koropatkin, N. M., Cameron, E. A. & Martens, E. C. How glycan metabolism shapes the human gut microbiota. *Nat. Rev. Microbiol.* **10,** 323–335 (2012).
42. Ravcheev, D. A., Godzik, A., Osterman, A. L. & Rodionov, D. A. Polysaccharides utilization in human gut bacterium Bacteroides thetaiotaomicron: comparative genomics reconstruction of metabolic and regulatory networks. *BMC Genomics* **14,** 873 (2013).
43. Comstock, L. E. *et al.* Analysis of a capsular polysaccharide biosynthesis locus of Bacteroides fragilis. *Infect. Immun.* **67,** 3525–3532 (1999).
44. Zitomersky, N. L., Coyne, M. J. & Comstock, L. E. Longitudinal analysis of the prevalence, maintenance, and IgA response to species of the order Bacteroidales in the human gut. *Infect. Immun.* **79,** 2012–2020 (2011).
45. Wu, M. *et al.* Genetic determinants of in vivo fitness and diet responsiveness in multiple human gut Bacteroides. *Science* **350,** aac5992 (2015).
46. Patrick, S. *et al.* Twenty-eight divergent polysaccharide loci specifying within- and amongst-strain capsule diversity in three strains of Bacteroides fragilis. *Microbiology* **156,** 3255–3269 (2010).
47. Coyne, M. J., Chatzidaki-Livanis, M., Paoletti, L. C. & Comstock, L. E. Role of glycan synthesis in colonization of the mammalian gut by the bacterial symbiont Bacteroides fragilis. *Proceedings of the National Academy of Sciences* **105,** 13099–13104 (2008).
48. Xu, J. *et al.* Evolution of symbiotic bacteria in the distal human intestine. *PLoS Biol.* **5,** e156 (2007).
49. Albenberg, L. *et al.* Correlation between intraluminal oxygen gradient and radial partitioning of intestinal microbiota. *Gastroenterology* **147,** 1055–63.e8 (2014).
50. Duncan, S. H., Hold, G. L., Harmsen, H. J. M., Stewart, C. S. & Flint, H. J. Growth requirements and fermentation products of Fusobacterium prausnitzii, and a proposal to reclassify it as Faecalibacterium prausnitzii gen. nov., comb. nov. *Int. J. Syst. Evol. Microbiol.* **52,** 2141–2146 (2002).
51. Browne, H. P. *et al.* Culturing of 'unculturable' human microbiota reveals novel taxa and extensive sporulation. *Nature* **533,** 543–546 (2016).
52. Berendsen, E. M., Boekhorst, J., Kuipers, O. P. & Wells-Bennik, M. H. J. A mobile genetic element profoundly increases heat resistance of bacterial spores. *ISME J.* **10,** 2633–2642 (2016).
53. Sommer, M. O. A., Church, G. M. & Dantas, G. The human microbiome harbors a diverse reservoir of antibiotic resistance genes. *Virulence* **1,** 299–303 (2010).
54. Whittle, G., Hund, B. D., Shoemaker, N. B. & Salyers, A. A. Characterization of the 13-kilobase ermF region of the Bacteroides conjugative transposon CTnDOT. *Appl. Environ. Microbiol.* **67,** 3488–3495 (2001).
55. Garnier, F., Taourit, S., Glaser, P., Courvalin, P. & Galimand, M. Characterization of transposon Tn1549, conferring VanB-type resistance in Enterococcus spp. *Microbiology* **146 (Pt 6),** 1481–1489 (2000).
56. Napolitano, M. G., Almagro-Moreno, S. & Boyd, E. F. Dichotomy in the evolution of pathogenicity island and bacteriophage encoded integrases from pathogenic Escherichia coli strains. *Infect. Genet. Evol.* **11,** 423–436 (2011).
57. Van Houdt, R., Leplae, R., Lima-Mendez, G., Mergeay, M. & Toussaint, A. Towards a more

638 accurate annotation of tyrosine-based site-specific recombinases in bacterial genomes. *Mob. DNA* **3,**
639 6 (2012).
640 58. Whittle, G., Hamburger, N., Shoemaker, N. B. & Salyers, A. A. A bacteroides conjugative
641 transposon, CTnERL, can transfer a portion of itself by conjugation without excising from the
642 chromosome. *J. Bacteriol.* **188,** 1169–1174 (2006).
643 59. Truong, D. T. *et al.* MetaPhlAn2 for enhanced metagenomic taxonomic profiling. *Nat. Methods* **12,**
644 902–903 (2015).
645 60. Wood, D. E. & Salzberg, S. L. Kraken: ultrafast metagenomic sequence classification using exact
646 alignments. *Genome Biol.* **15,** R46 (2014).
647 61. Ounit, R., Wanamaker, S., Close, T. J. & Lonardi, S. CLARK: fast and accurate classification of
648 metagenomic and genomic sequences using discriminative k-mers. *BMC Genomics* **16,** 236 (2015).
649 62. Ahn, T.-H., Chai, J. & Pan, C. Sigma: strain-level inference of genomes from metagenomic analysis
650 for biosurveillance. *Bioinformatics* **31,** 170–177 (2015).
651 63. Luo, C. *et al.* ConStrains identifies microbial strains in metagenomic datasets. *Nat. Biotechnol.* **33,**
652 1045–1052 (2015).
653 64. Greenblum, S., Carr, R. & Borenstein, E. Extensive strain-level copy-number variation across human
654 gut microbiome species. *Cell* **160,** 583–594 (2015).
655 65. Nayfach, S., Rodriguez-Mueller, B., Garud, N. & Pollard, K. S. An integrated metagenomics
656 pipeline for strain profiling reveals novel patterns of bacterial transmission and biogeography.
657 *Genome Res.* **26,** 1612–1625 (2016).
658 66. Smit, A., Hubley, R. & Green, P. RepeatMasker Open-4.0. 2013--2015. *Institute for Systems*
659 *Biology. http://repeatmasker. org* (2015).
660 67. Bao, W., Kojima, K. K. & Kohany, O. Repbase Update, a database of repetitive elements in
661 eukaryotic genomes. *Mob. DNA* **6,** 11 (2015).
662 68. Antibiotic / Antimicrobial Resistance | CDC. Available at:
663 https://www.cdc.gov/drugresistance/index.html. (Accessed: 14th June 2017)
664 69. Caballero, S. *et al.* Cooperating Commensals Restore Colonization Resistance to Vancomycin-
665 Resistant Enterococcus faecium. *Cell Host Microbe* **21,** 592–602.e4 (2017).
666 70. Mimee, M., Tucker, A. C., Voigt, C. A. & Lu, T. K. Programming a Human Commensal Bacterium,
667 Bacteroides thetaiotaomicron, to Sense and Respond to Stimuli in the Murine Gut Microbiota. *Cell*
668 *Syst* **1,** 62–71 (2015).
669 71. Liu, Y.-J., Zhang, J., Cui, G.-Z. & Cui, Q. Current progress of targetron technology: development,
670 improvement and application in metabolic engineering. *Biotechnol. J.* **10,** 855–865 (2015).
671 72. Ondov, B. D. *et al.* Mash: fast genome and metagenome distance estimation using MinHash.
672 *Genome Biol.* **17,** 132 (2016).
673 73. Li, H. & Durbin, R. Fast and accurate short read alignment with Burrows–Wheeler transform.
674 *Bioinformatics* **25,** 1754–1760 (2009).
675 74. Hyatt, D. *et al.* Prodigal: prokaryotic gene recognition and translation initiation site identification.
676 *BMC Bioinformatics* **11,** 119 (2010).
677 75. Jones, P. *et al.* InterProScan 5: genome-scale protein function classification. *Bioinformatics* **30,**
678 1236–1240 (2014).
679 76. Fouts, D. E. Phage_Finder: automated identification and classification of prophage regions in
680 complete bacterial genome sequences. *Nucleic Acids Res.* **34,** 5839–5851 (2006).
681 77. Abby, S. S. *et al.* Identification of protein secretion systems in bacterial genomes. *Sci. Rep.* **6,** 23080
682 (2016).
683 78. Kurtz, S. *et al.* Versatile and open software for comparing large genomes. *Genome Biol.* **5,** R12
684 (2004).
685 79. Katoh, K. & Standley, D. M. MAFFT multiple sequence alignment software version 7:
686 improvements in performance and usability. *Mol. Biol. Evol.* **30,** 772–780 (2013).
687 80. Capella-Gutiérrez, S., Silla-Martínez, J. M. & Gabaldón, T. trimAl: a tool for automated alignment
688 trimming in large-scale phylogenetic analyses. *Bioinformatics* **25,** 1972–1973 (2009).

81. Stamatakis, A. RAxML version 8: a tool for phylogenetic analysis and post-analysis of large phylogenies. *Bioinformatics* **30,** 1312–1313 (2014).
82. Revell, L. J. Phytools: Phylogenetic tools or comparative biology (and other things). (2011).
83. Johnson, L. S., Eddy, S. R. & Portugaly, E. Hidden Markov model speed heuristic and iterative HMM search procedure. *BMC Bioinformatics* **11,** 431 (2010).
84. Beissbarth, T. & Speed, T. P. GOstat: find statistically overrepresented Gene Ontologies within a group of genes. *Bioinformatics* **20,** 1464–1465 (2004).
85. Yu, G., Wang, L.-G., Han, Y. & He, Q.-Y. clusterProfiler: an R package for comparing biological themes among gene clusters. *OMICS* **16,** 284–287 (2012).

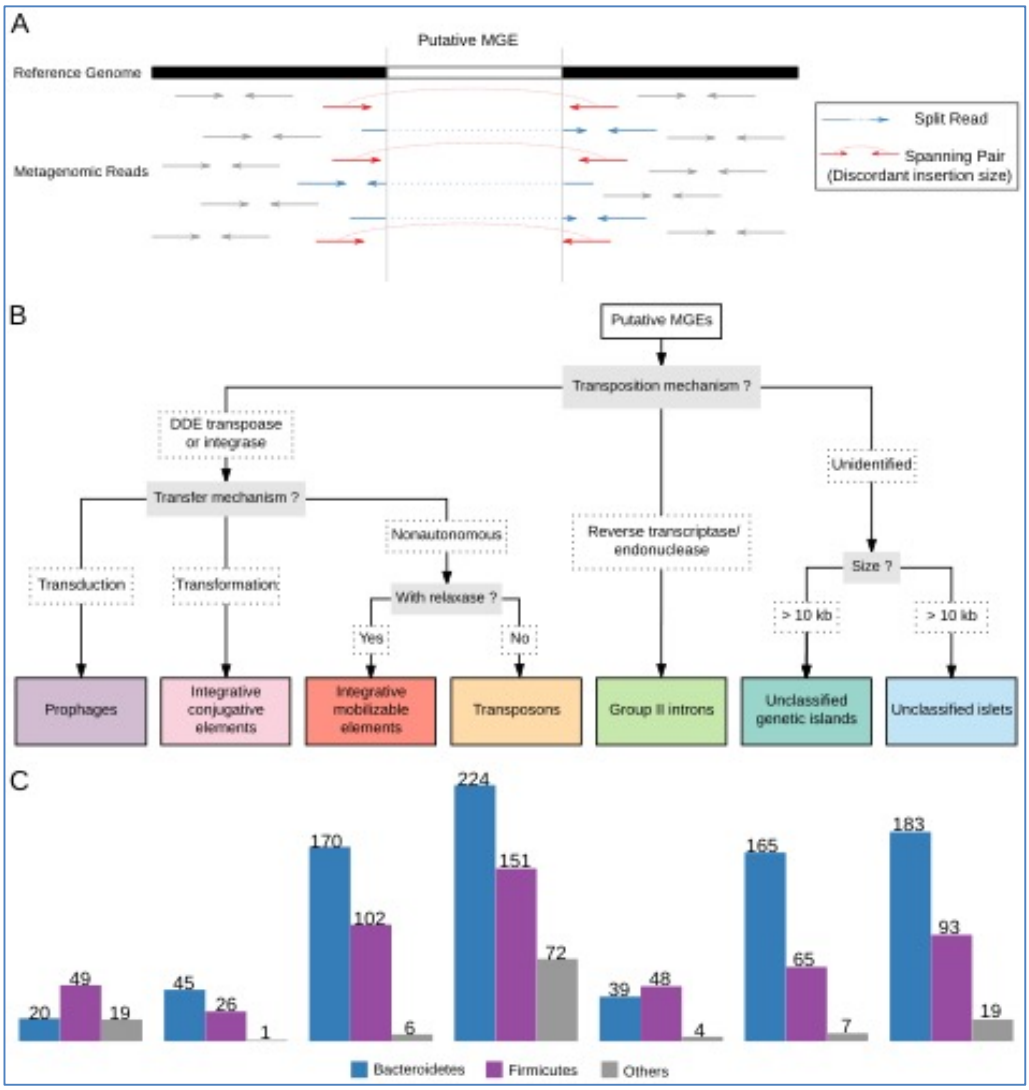

Figure 1 | Identification and classification of gut microbiome MGEs. (A) The method used to identify putative MGEs using split reads and discordantly-mapped paired-end reads. Split reads are colored blue, and discordantly-mapped paired-end reads are colored red. (B) The method used to classify MGEs based on gene signatures. (C) The number of MGE clusters identified stratified by phyla and MGE classification.

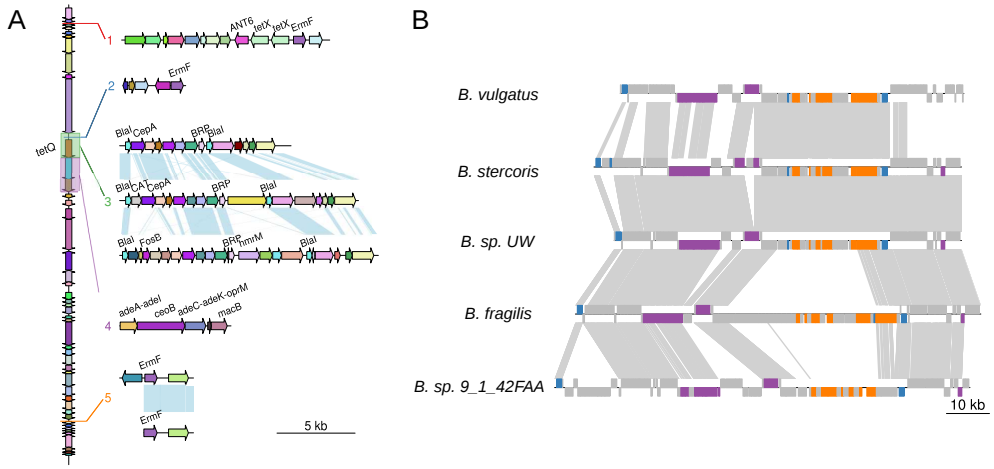

Figure 2 | Examples of niche-adaptive genes. (A) CTn-DOT-like elements have acquired antibiotic resistance genes on multiple, independent occasions. Here, we show insertion sites of antibiotic resistant genes in CTnDOT-like elements. A CTnDOT-like ICE is shown on the left. Orthologs between elements are visualized using genoPlotR (light blue connections) and are the same color. Numbers in the top panel represent the insertion site of the numbered elements below. Antibiotic resistance genes are labeled. (B) ICEs are involved in the transfer of capsular polysaccharide biosynthesis loci between Bacteroidetes species. Here, we show examples of ICEs containing capsular polysaccharide biosynthesis loci. Orthologs between elements are plotted with GenoPlotR. Genes involved in capsular polysaccharide biosynthesis are colored orange, integrases are colored blue, and genes involved in conjugation are colored purple. Grey links indicate orthologs between elements.

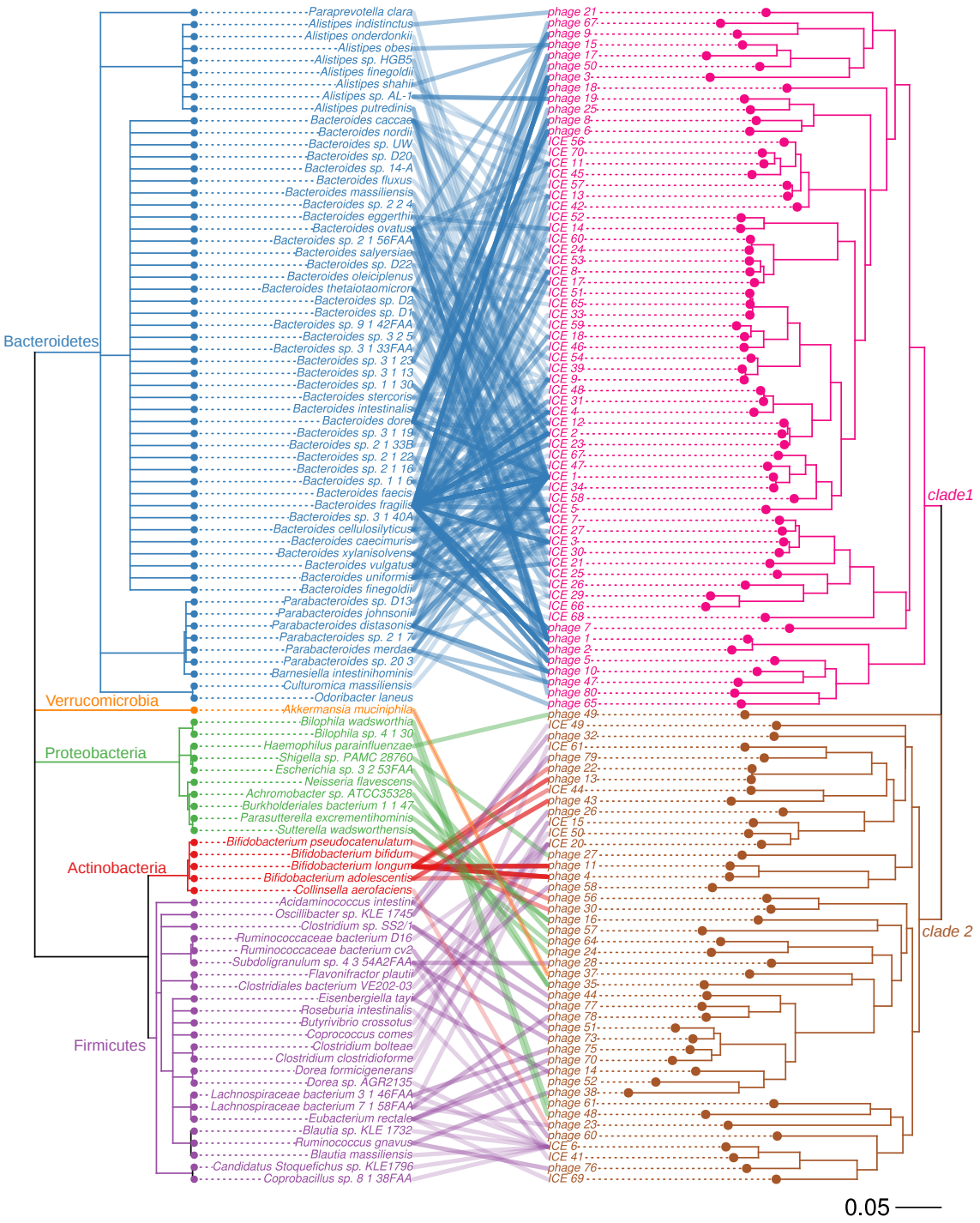

Figure 3 | Tanglegram of host species lineages and phylogeny of the integrases in prophages and ICEs. A tanglegram of tyrosine integrases from ICEs and prophages with the species phylogeny plotted on the left and tyrosine integrase phylogeny plotted on the right. Connections are drawn between a species and the tyrosine integrase(s) found in that species and each connecting line is colored according to host bacteria phylum.

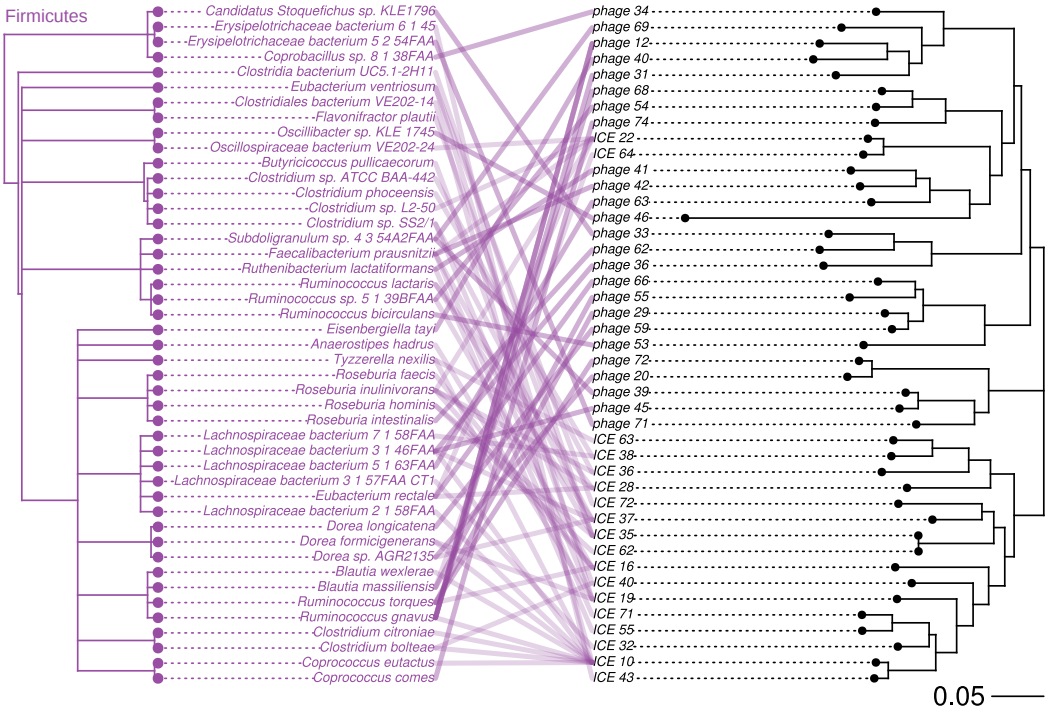

Figure 4 | Tanglegram of host species lineages and phylogeny of serine integrases in prophages and ICEs. A tanglegram of serine integrases from ICEs and prophages with the species phylogeny plotted on the left and tyrosine integrase phylogeny plotted on the right. Connections are drawn between a species and the serine integrase(s) found in that species.

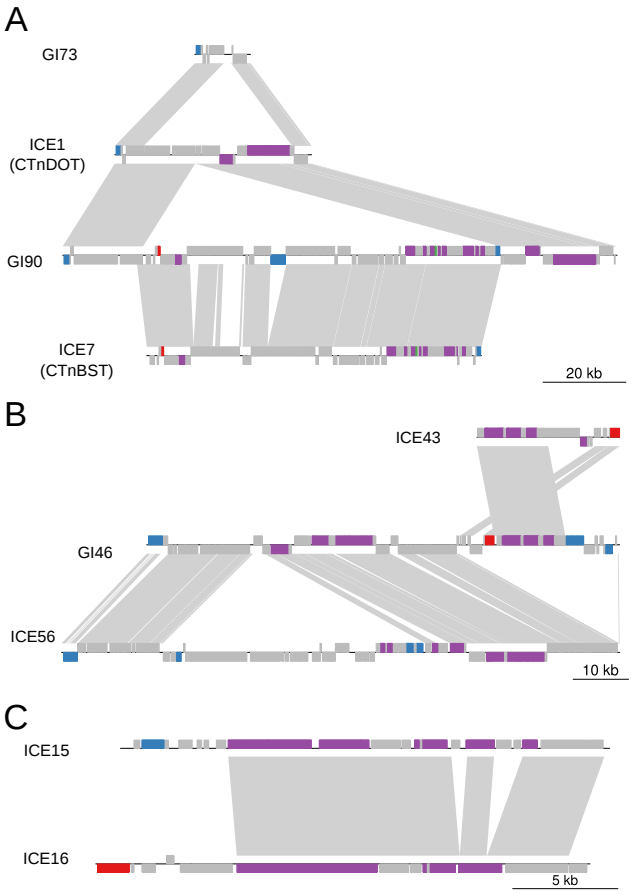

722 **Figure 5 | Modular evolution of MGEs.** Examples of deletion, acquisition, and exchange of gene
723 modules between MGEs. Orthologous genes between elements are shown with grey connections and are
724 plotted with genoPlotR. Tyrosine integrases are colored blue, serine integrases are colored red, and genes
725 involved in conjugation are colored purple. (A) GI73 was likely formed via a deletion of a CTnDOT-like
726 ICE. GI90 was formed from an insertion of the ICE CTnBST into a CTnDOT-like ICE to form a large,
727 composite GI that transfers as a unit. (B) An example of the tandem insertion of two ICEs to form a larger
728 GI that moves as a unit. (C) An example of recombination module exchanges between ICE15 and ICE16.

729 ## Supplementary information

730 **Supplementary Figure 1:** Classification of gut microbiome MGEs at the phylum level

731 **Supplementary Figure 2:** Tanglegram of host species lineages and phylogeny of group II intron proteins

732 **Supplementary Table 1:** Antibiotic resistant genes identified in MGEs classes

733 ## Supplementary Tables and Data

734 **Supplementary Table 2**: Annotation and classification of MGEs (xlsx)

735 **Supplementary Table 3**: Niche adaptive cargo genes (xlsx)

736 **Supplementary Table 4**: Enrichment analysis of cargo genes (xlsx)

737 **Supplementary Table 5**: Annotation of regions with ARG insertions in CTnDOT-like elements (xlsx)

738 **Supplementary Data 1**: MGE sequences (fasta)

739 **Supplementary Data 2**: Annotation of genes in MGEs (gff3)

740 **Supplementary Data 3**: Sequences of CTnDOT-like elements with ARG insertions (fasta)

741 **Supplementary Data 4:** Scripts to implement the SRID method and the genome assembly accession

742 numbers and HMP SRA accession numbers used in this study.(zipped txt)

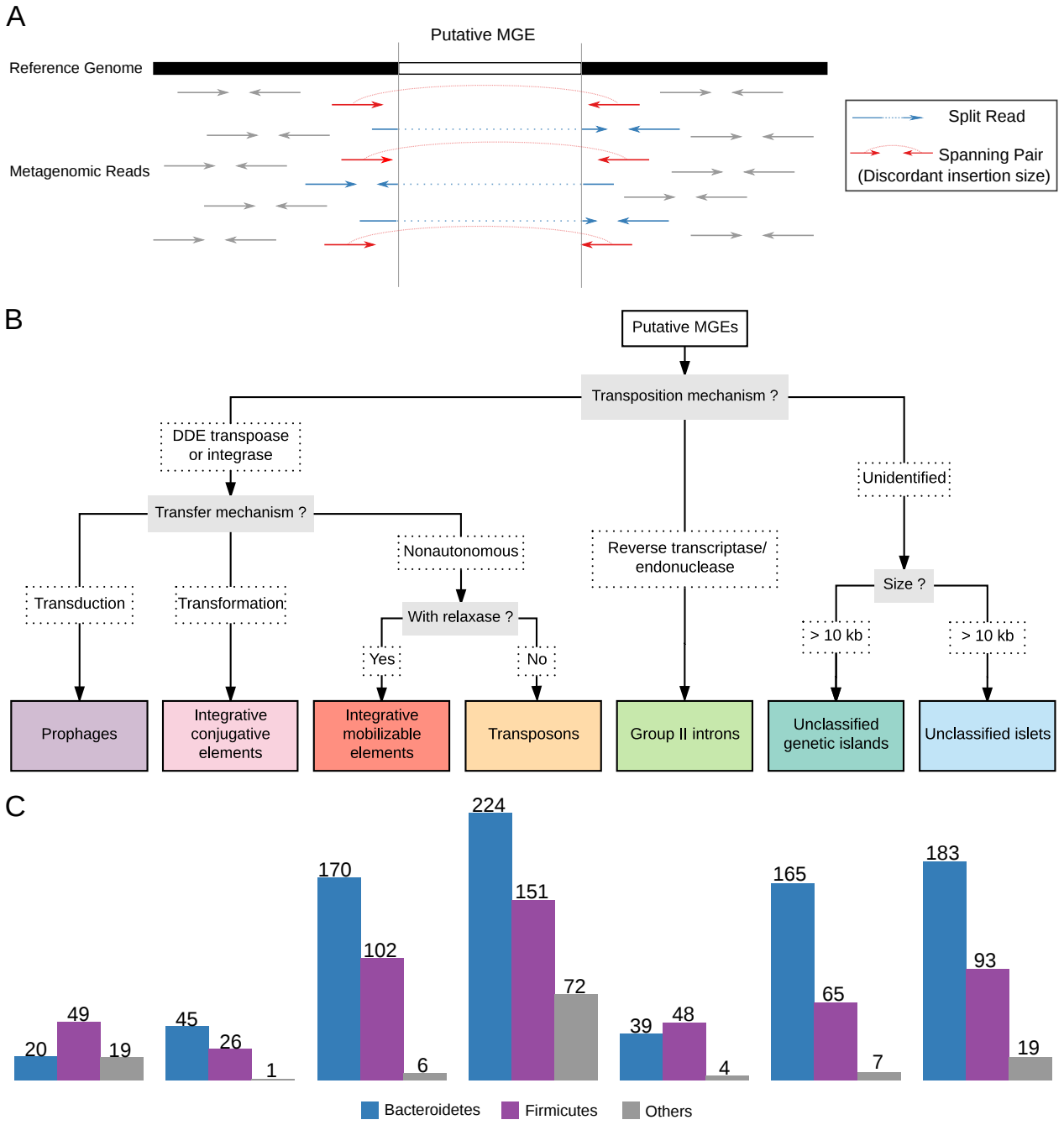
A
Putative MGE
Reference Genome
Metagenomic Reads
Split Read
Spanning Pair
(Discordant insertion size)
B
Putative MGEs
Transposition mechanism ?
DDE transpoase
or integrase
Transfer mechanism ?
Nonautonomous
Reverse transcriptase/
endonuclease
Unidentified
Size ?
Transduction
Transformation
With relaxase ?
Yes
No
> 10 kb
> 10 kb
Prophages
Integrative
conjugative
elements
Integrative
mobilizable
elements
Transposons
Group II introns
Unclassified
genetic islands
Unclassified islets
C
20
49
19
45
26
1
170
102
6
224
151
72
39
48
4
165
65
7
183
93
19
Bacteroidetes
Firmicutes
Others

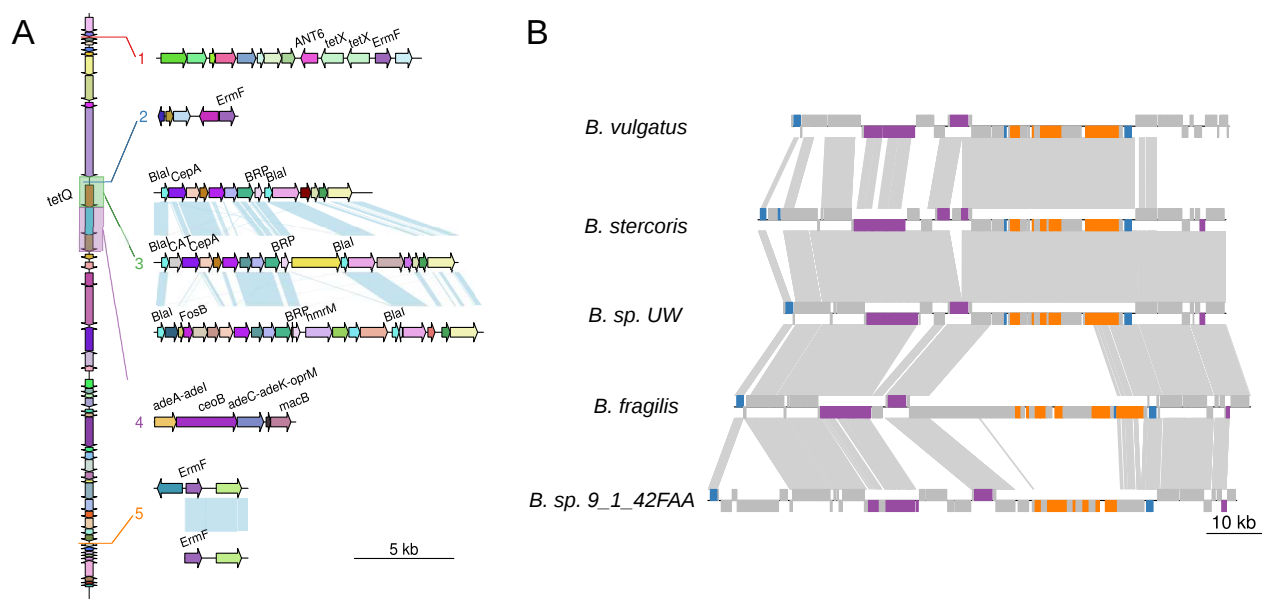
A
1
ANT6
tetX
tetX
ErmF
2
ErmF
tetQ
BlaI
CepA
BRP
BlaI
3
BlaI
CAT
CepA
BRP
BlaI
BlaI
FosB
BRP
hmrM
BlaI
4
adeA-adeI
ceoB
adeC-adeK-oprM
macB
5
ErmF
ErmF
5 kb
B
B. vulgatus
B. stercoris
B. sp. UW
B. fragilis
B. sp. 9_1_42FAA
10 kb

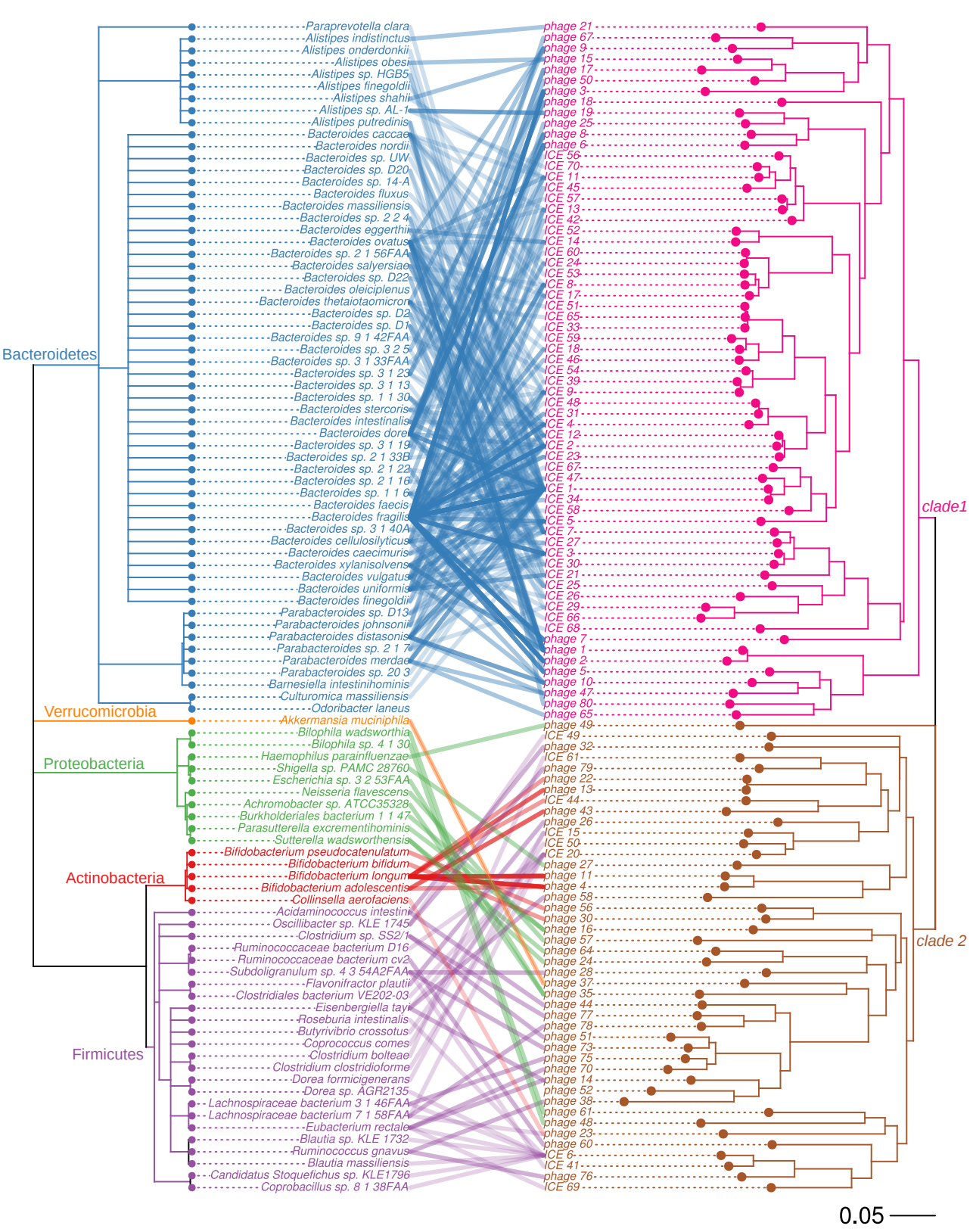
Bacteroidetes
Verrucomicrobia
Proteobacteria
Actinobacteria
Firmicutes
Paraprevotella clara
Alistipes indistinctus
Alistipes onderdonkii
Alistipes obesi
Alistipes sp. HGB5
Alistipes finegoldii
Alistipes shahii
Alistipes sp. AL-1
Alistipes putredinis
Bacteroides caccae
Bacteroides nordii
Bacteroides sp. UW
Bacteroides sp. D20
Bacteroides sp. 14-A
Bacteroides fluxus
Bacteroides massiliensis
Bacteroides sp. 2 2 4
Bacteroides eggerthii
Bacteroides ovatus
Bacteroides sp. 2 1 56FAA
Bacteroides salyersiae
Bacteroides sp. D22
Bacteroides oleiciplenus
Bacteroides thetaiotaomicron
Bacteroides sp. D2
Bacteroides sp. D1
Bacteroides sp. 9 1 42FAA
Bacteroides sp. 3 2 5
Bacteroides sp. 3 1 33FAA
Bacteroides sp. 3 1 23
Bacteroides sp. 3 1 13
Bacteroides sp. 1 1 30
Bacteroides stercoris
Bacteroides intestinalis
Bacteroides dorei
Bacteroides sp. 3 1 19
Bacteroides sp. 2 1 33B
Bacteroides sp. 2 1 22
Bacteroides sp. 2 1 16
Bacteroides sp. 1 1 6
Bacteroides faecis
Bacteroides fragilis
Bacteroides sp. 3 1 40A
Bacteroides cellulosilyticus
Bacteroides caecimuris
Bacteroides xylanisolvens
Bacteroides vulgatus
Bacteroides uniformis
Bacteroides finegoldii
Parabacteroides sp. D13
Parabacteroides johnsonii
Parabacteroides distasonis
Parabacteroides sp. 2 1 7
Parabacteroides merdae
Parabacteroides sp. 20 3
Barnesiella intestinihominis
Culturomica massiliensis
Odoribacter laneus
Akkermansia muciniphila
Bilophila wadsworthia
Bilophila sp. 4 1 30
Haemophilus parainfluenzae
Shigella sp. PAMC 28760
Escherichia sp. 3 2 53FAA
Neisseria flavescens
Achromobacter sp. ATCC35328
Burkholderiales bacterium 1 1 47
Parasutterella excrementihominis
Sutterella wadsworthensis
Bifidobacterium pseudocatenulatum
Bifidobacterium bifidum
Bifidobacterium longum
Bifidobacterium adolescentis
Collinsella aerofaciens
Acidaminococcus intestini
Oscillibacter sp. KLE 1745
Clostridium sp. SS2/1
Ruminococcaceae bacterium D16
Ruminococcaceae bacterium cv2
Subdoligranulum sp. 4 3 54A2FAA
Flavonifractor plautii
Clostridiales bacterium VE202-03
Eisenbergiella tayi
Roseburia intestinalis
Butyrivibrio crossotus
Coprococcus comes
Clostridium bolteae
Clostridium clostridioforme
Dorea formicigenerans
Dorea sp. AGR2135
Lachnospiraceae bacterium 3 1 46FAA
Lachnospiraceae bacterium 7 1 58FAA
Eubacterium rectale
Blautia sp. KLE 1732
Ruminococcus gnavus
Blautia massiliensis
Candidatus Stoquefichus sp. KLE1796
Coprobacillus sp. 8 1 38FAA
phage 21
phage 67
phage 9
phage 15
phage 17
phage 50
phage 3
phage 18
phage 19
phage 25
phage 8
phage 6
ICE 56
ICE 70
ICE 11
ICE 45
ICE 57
ICE 13
ICE 42
ICE 52
ICE 14
ICE 60
ICE 24
ICE 53
ICE 8
ICE 17
ICE 51
ICE 65
ICE 33
ICE 59
ICE 18
ICE 46
ICE 54
ICE 39
ICE 9
ICE 48
ICE 31
ICE 4
ICE 12
ICE 2
ICE 23
ICE 67
ICE 47
ICE 1
ICE 34
ICE 58
ICE 5
ICE 7
ICE 27
ICE 3
ICE 30
ICE 21
ICE 25
ICE 26
ICE 29
ICE 66
ICE 68
phage 7
phage 1
phage 2
phage 5
phage 10
phage 47
phage 80
phage 65
phage 49
ICE 49
phage 32
ICE 61
phage 79
phage 22
phage 13
ICE 44
phage 43
phage 26
ICE 15
ICE 50
ICE 20
phage 27
phage 11
phage 4
phage 58
phage 56
phage 30
phage 16
phage 57
phage 64
phage 24
phage 28
phage 37
phage 35
phage 44
phage 77
phage 78
phage 51
phage 73
phage 75
phage 70
phage 14
phage 52
phage 38
phage 61
phage 48
phage 23
phage 60
ICE 6
ICE 41
phage 76
ICE 69
clade1
clade 2
0.05

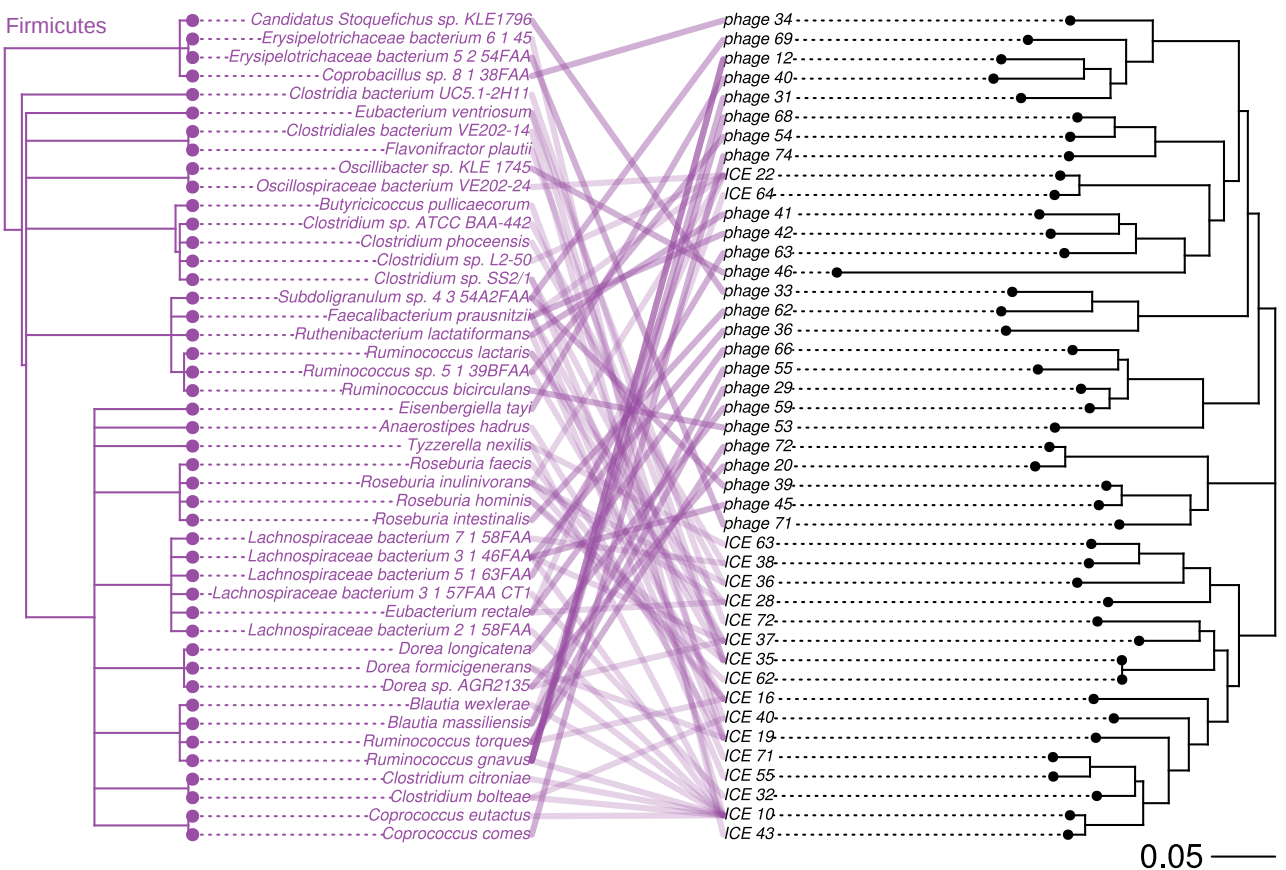
Firmicutes
Candidatus Stoquefichus sp. KLE1796
Erysipelotrichaceae bacterium 6 1 45
Erysipelotrichaceae bacterium 5 2 54FAA
Coprobacillus sp. 8 1 38FAA
Clostridia bacterium UC5.1-2H11
Eubacterium ventriosum
Clostridiales bacterium VE202-14
Flavonifractor plautii
Oscillibacter sp. KLE 1745
Oscillospiraceae bacterium VE202-24
Butyricicoccus pullicaecorum
Clostridium sp. ATCC BAA-442
Clostridium phoceensis
Clostridium sp. L2-50
Clostridium sp. SS2/1
Subdoligranulum sp. 4 3 54A2FAA
Faecalibacterium prausnitzii
Ruthenibacterium lactatiformans
Ruminococcus lactaris
Ruminococcus sp. 5 1 39BFAA
Ruminococcus bicirculans
Eisenbergiella tayi
Anaerostipes hadrus
Tyzzerella nexilis
Roseburia faecis
Roseburia inulinivorans
Roseburia hominis
Roseburia intestinalis
Lachnospiraceae bacterium 7 1 58FAA
Lachnospiraceae bacterium 3 1 46FAA
Lachnospiraceae bacterium 5 1 63FAA
Lachnospiraceae bacterium 3 1 57FAA CT1
Eubacterium rectale
Lachnospiraceae bacterium 2 1 58FAA
Dorea longicatena
Dorea formicigenerans
Dorea sp. AGR2135
Blautia wexlerae
Blautia massiliensis
Ruminococcus torques
Ruminococcus gnavus
Clostridium citroniae
Clostridium bolteae
Coprococcus eutactus
Coprococcus comes
phage 34
phage 69
phage 12
phage 40
phage 31
phage 68
phage 54
phage 74
ICE 22
ICE 64
phage 41
phage 42
phage 63
phage 46
phage 33
phage 62
phage 36
phage 66
phage 55
phage 29
phage 59
phage 53
phage 72
phage 20
phage 39
phage 45
phage 71
ICE 63
ICE 38
ICE 36
ICE 28
ICE 72
ICE 37
ICE 35
ICE 62
ICE 16
ICE 40
ICE 19
ICE 71
ICE 55
ICE 32
ICE 10
ICE 43
0.05

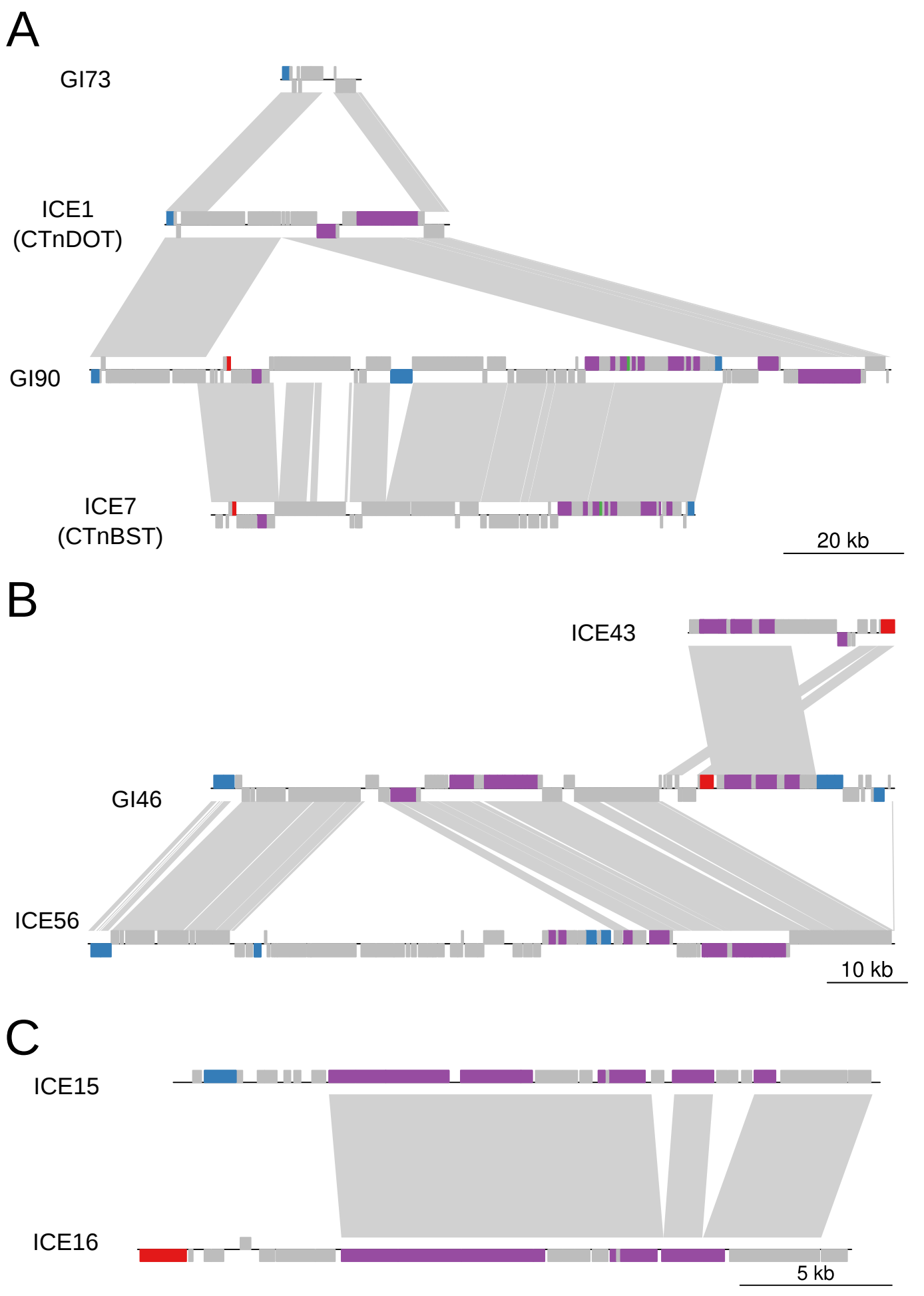
A
GI73
ICE1
(CTnDOT)
GI90
ICE7
(CTnBST)
20 kb
B
ICE43
GI46
ICE56
10 kb
C
ICE15
ICE16
5 kb